

Accepted version

Licence CC BY-NC-ND

Please cite as:

Jademilson Celestino dos Santos, Amanda Bernardes, Letizia Giampietro, Alessandra Ammazalorso, Barbara De Filippis, Rosa Amoroso, Igor Polikarpov (2015), Different binding and recognition modes of GL479, a dual agonist of Peroxisome Proliferator-Activated Receptor  $\alpha/\gamma$ , *Journal of Structural Biology* 191 (2015) 332–340  
doi: <http://dx.doi.org/10.1016/j.jsb.2015.07.006>

# Different binding and recognition modes of GL479, a dual agonist of Peroxisome Proliferator-Activated Receptor $\alpha/\gamma$

Jademilson Celestino dos Santos <sup>a</sup>, Amanda Bernardes <sup>a</sup>, Letizia Giampietro <sup>b</sup>, Alessandra Ammazalorso <sup>b</sup>, Barbara De Filippis <sup>b</sup>, Rosa Amoroso <sup>b</sup>, Igor Polikarpov <sup>a,\*</sup>

<sup>a</sup> Grupo de Biotecnologia Molecular, Instituto de Física de São Carlos, Universidade de São Paulo, São Carlos, SP 13566-590, Brazil

<sup>b</sup> Dipartimento di Farmacia, Università degli Studi 'G. d'Annunzio', via dei Vestini 31, 66100 Chieti, Italy

## abstract

Peroxisome Proliferator-Activated Receptors (PPARs) are ligand-dependent transcription factors that control various functions in human organism, including the control of glucose and lipid metabolism. PPAR $\gamma$  is a target of TZD agonists, clinically used to improve insulin sensitivity whereas fibrates, PPAR $\alpha$  ligands, lower serum triglyceride levels. We report here the structural studies of GL479, a synthetic dual PPAR $\alpha/\gamma$  agonist, designed by a combination of clofibric acid skeleton and a phenyldiazenyl moiety, as bioisosteric replacement of stilbene group, in complex with both PPAR $\alpha$  and PPAR $\gamma$  receptors. GL479 was previously reported as a partial agonist of PPAR $\gamma$  and a full agonist of PPAR $\alpha$  with high affinity for both PPARs. Our structural studies reveal different binding modes of GL479 to PPAR $\alpha$  and PPAR $\gamma$ , which may explain the distinct activation behaviors observed for each receptor. In both cases the ligand interacts with a Tyr located at helix 12 (H12), resulting in the receptor active conformation. In the complex with PPAR $\alpha$ , GL479 occupies the same region of the ligand-binding pocket (LBP) observed for other full agonists, whereas GL479 bound to PPAR $\gamma$  displays a new binding mode. Our results indicate a novel region of PPARs LBP that may be explored for the design of partial agonists as well dual PPAR $\alpha/\gamma$  agonists that combine, simultaneously, the therapeutic effects of the treatment of insulin resistance and dyslipidemia.

## 1. Introduction

The lifestyle of the 21st century, characterized by people sedentary routine and diets rich in fat and carbohydrates, has contributed to an increase in the occurrence of metabolic syndromes, including type 2 diabetes mellitus, dyslipidemia, obesity and other cardiovascular diseases (Eckel et al., 2005). Several of the metabolic pathways involved in these disorders are regulated by Peroxisome Proliferator-Activated Receptors (PPARs), which are members of the superfamily of the nuclear receptors and function as transcription factors activated by several synthetic and natural ligands (Forman et al., 1997). These receptors form

heterodimers with the Retinoid X Receptor (RXR) and the heterodimerization is essential for the recruitment of coregulators and consequent initiation of transcription (Auwerx, 1999; Berger and Moller, 2002; Michalik et al., 2006; Rastinejad et al., 2015). There are three PPAR isotypes, encoded by distinct genes and designated as PPAR $\alpha$ , PPAR $\beta/\delta$  and PPAR $\gamma$ . PPAR $\alpha$  is expressed predominantly in metabolically active tissues, including liver, adipose tissue, kidney and heart. PPAR $\beta/\delta$  expression occurs in a wide variety of tissues and cells, with relatively higher levels in adipose tissue, brain, liver and skin. PPAR $\gamma$  expression is abundant in fatty tissues, liver and heart (Auwerx, 1999; Auwerx et al., 2003; Kota et al., 2005).

Among the three isotypes, PPAR $\alpha$  and PPAR $\gamma$  have been the most widely studied, as they have important roles in regulating glucose, lipids and cholesterol metabolism as well as in the fatty acid  $\beta$ -oxidation and homeostasis. It makes these receptors important pharmacological targets of the drugs used for treatment of type 2 diabetes mellitus (T2DM) and dyslipidemia (Harmon et al., 2011; Mandard et al., 2004). The PPAR $\alpha$  is a molecular target for fibrates, a class of hypolipidemic drugs used in the treatment of

**Abbreviations:** PPAR, Peroxisome Proliferator-Activated Receptor; LBD, ligand binding domain; DMSO, dimethyl sulfoxide; GL479, (E)-2-methyl-2-(4-(2-(4-(phenyldiazenyl)phenoxy)ethyl)phenoxy)propanoic acid; DTT, dithiothreitol; IPTG, Isopropyl  $\beta$ -D-1-thiogalactopyranoside; HDL, high density lipoprotein; LBP, ligand binding pocket.

\* Corresponding author.

E-mail address: ipolikarpov@ifsc.usp.br (I. Polikarpov).

dyslipidemia in humans. PPAR $\alpha$  activation by fibrates decreases triglyceride levels, while increasing HDL cholesterol via metabolism control of fatty acids and lipoproteins. Clinical studies have also demonstrated that fibrates reduce the incidence of atherosclerosis and cardiovascular events. Additionally, activation of PPAR $\alpha$  produces an increased sensitivity to insulin and glucose tolerance in patients with T2DM. Fibrates are well tolerated by most patients, however some adverse effects have been reported, mostly gastrointestinal, but also anxiety, headache, dizziness, sleep disorder, rash and hives. Because fibrate metabolism and excretion are mainly performed by the kidneys, patients with kidney problems are advised not to use them (Barter and Rye, 2008). PPAR $\gamma$  is the molecular targets of several marketed drugs, mostly the thiazolidinediones (TZDs) that were developed mainly to have high affinity and full agonism towards this receptor subtype (Henke et al., 1998). These pharmaceutical molecules increase insulin sensitivity and are used clinically for the treatment of T2DM, which is associated with various metabolic disorders including obesity, hypertension and dyslipidemia. Albeit their antidiabetic effect, the TZDs present risks to the patients (Levinet et al., 2015); troglitazone was withdrawn from the market for causing hepatotoxicity, while rosiglitazone has a restricted use because of the greater risk of death from cardiovascular events. Currently, only pioglitazone is in unrestricted use, however many adverse effects are attributed to the continued use of pioglitazone, such as increased incidence of bone fractures distal, fluid retention, weight gain and increased occurrence of heart failure (Inzucchi et al., 2015; Nathan et al., 2009). The undesirable side effects attributed to the TZDs appear to be linked to the full activation (full agonists) of gene expression in diverse tissues, which is related to non-specificity of this class of ligands (Liu et al., 2015). Consistent with this notion, some of the non-TZD ligands, that are also full agonists with antidiabetic activity, exhibited similar side effects (Liu et al., 2015). Therefore, a promising approach for the development of PPAR $\gamma$  agonists, with an acceptable safety profile, is the search for agonists that partially modulate PPAR $\gamma$  target genes (Argmann et al., 2005; Cock et al., 2004; Liu et al., 2015). Despite weak receptor activation, partial PPAR $\gamma$  agonists may have a higher selectivity and fewer side effects (Choi et al., 2010). Structurally, full agonists generally make interactions with residues of H12, whereas partial agonists stabilize other regions of the ligand binding pocket (LBP), without direct contact with the H12 (Bruning et al., 2007).

A challenge to activate both PPAR $\alpha$  and PPAR $\gamma$  with a single drug, thus simultaneously normalizing glucose and lipids levels, has led to intensive research efforts. Several PPAR $\alpha/\gamma$  dual agonists, such as muraglitazar, ragaglitazar, tesaglitazar, and aleglitazar, have been synthesized and tested in clinical phase 2 or 3 (Fiévet et al., 2006). Most of these tests have been canceled because of the pronounced side effects of the tested dual agonists. This situation might arise from the fact that all cited glitazars have significantly higher affinity to PPAR $\gamma$  than to PPAR $\alpha$  and some of them can be considered as pure PPAR $\gamma$  agonists. When fenofibric acid and rosiglitazone were used as controls of PPAR $\alpha$  and PPAR $\gamma$  activity, respectively, some glitazars (muraglitazar and farglitazar, for example) were significantly more potent to PPAR $\gamma$  than a rosiglitazone, when administered in clinically prescribed doses (Fiévet et al., 2006). Nevertheless, better dual agonists, developed to increase insulin sensitivity and concurrently prevent diabetic cardiovascular complications, still offer a very attractive therapeutic option, particularly if the compounds are able to combine an intermediate to higher PPAR $\alpha$  affinity with a selective PPAR $\gamma$ -modulating capacity (Fiévet et al., 2006). Aiming to contribute to better understanding of a structural basis of full and partial activation of PPARs, here we present the structures of the ligand binding domain (LBD) of PPAR $\alpha$  and PPAR $\gamma$  complexed

with GL479, a PPAR $\alpha/\gamma$  dual agonist (Fig. 1A). This compound was synthesized by Giampietro and colleagues in the search for novel PPAR ligands based on a combination of two key pharmacophores: the clofibric acid skeleton and natural products as stilbene, chalcone, and their bioisosters (Giampietro et al., 2012). The aim of this project was to improve the pharmacological activity of classical fibrates by introducing the antioxidant, antilipidemic and antiplatelet properties of natural scaffolds. The introduction of a diazenyl function spaced by a three atom linker from clofibric acid resulted in GL479, a good PPAR  $\alpha/\gamma$  agonist (PPAR $\alpha$  EC<sub>50</sub> = 0.6  $\mu$ M, PPAR $\gamma$  EC<sub>50</sub> = 1.4  $\mu$ M). GL479 was also able to influence the gene expression of CPT1A, an enzyme involved in lipid metabolism in liver, related with long-chain fatty acid transport into hepatocyte mitochondria (Giampietro et al., 2012). Our present crystallographic studies revealed that GL479 interacts with ligand binding pocket (LBP) of both PPAR $\alpha$  and PPAR $\gamma$  but displays different binding modes. Considering the fact that GL479 acts as a full agonist of PPAR $\alpha$  and partial agonist of PPAR $\gamma$ , we advocate that the observed differences in the binding modes are directly related to the efficacy of the PPARs activation by the ligand. Additionally, our structural analysis offers clues for amelioration of the ligands design for pharmaceutical applications, aimed to simultaneously activate more than one PPAR isoform.

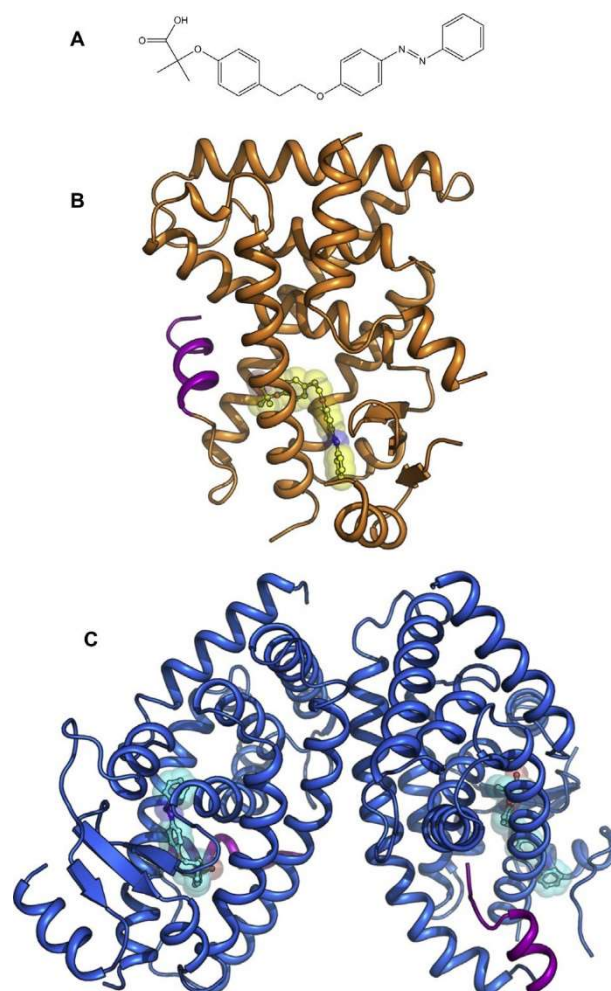


**Fig. 1.** Structures of PPAR $\alpha$  and PPAR $\gamma$  LBDs bound to GL479. (A) Chemical structure of GL479 dual PPAR $\alpha/\gamma$  agonist. (B) An overall schematic representation of the PPAR $\alpha$ -LBD structure. The ligand GL479 is shown as a ball and stick model in yellow. (C) The PPAR $\gamma$ -LBD crystallized as an asymmetric unit containing active and inactive forms of the receptor. In both models the H12 is shown in purple.

## 2. Materials and methods

### 2.1. Protein expression and purification

The recombinant LBD of PPAR $\alpha$  (residues 195–468) and PPAR $\gamma$  (residues 193–441) were expressed and purified as previously described (Bernardes et al., 2013; Puhl et al., 2012). Briefly, PPAR $\alpha$ -LBD and PPAR $\gamma$ -LBD were cloned into pET28a (+) plasmid and introduced in competent cells of BL21 DE3 *Escherichia coli* strain. The transformed cells were cultured at 37 °C until OD<sub>600 nm</sub> reached 0.6. Protein expression was induced with 1 mM IPTG for 16 h at 18 °C. Cells were collected by centrifugation and disrupted by sonication. Following centrifugation to remove cell debris, purification of the His-tagged protein was conducted by metal affinity chromatography using a NiSO<sub>4</sub>-loaded HiTrap™5 mL column High Performance (GE Healthcare) pre-equilibrated with 10 mM imidazole, 20 mM Tris-HCl pH 7.5, 50 mM NaCl, 5% glycerol and 1 mM DTT. Clarified cell lysate were applied to the column followed by extensive washing with the same buffer, and subsequently the protein elution with a 10–500 mM gradient of imidazole. Each eluted sample was submitted to another step of protein purification using a Superdex 75 16/60 column (GE Healthcare) coupled to an AKTA Purifier (Amersham Bioscience) and equilibrated with the buffer 20 mM Tris-HCl pH 8.0, 1 mM DTT, 150 mM NaCl and 5% glycerol, at a continuous flow of 1 mL min<sup>-1</sup>. The His-tag was removed using thrombin proteolysis. The protein purity was monitored by SDS-PAGE stained with Coomassie Blue. Finally, complexes between PPAR $\alpha$ /PPAR $\gamma$  and GL479 were obtained by incubation of receptors at 15/10 mg mL<sup>-1</sup> with 3-fold/5-fold of GL479 excess, respectively.

### 2.2. Crystallization, data collection and structure determination

The crystals of both complexes were obtained using hanging drop vapor diffusion method, at 18 °C, mixing in the drops equal volumes of protein and reservoir solution (1  $\mu$ L of each). For PPAR $\alpha$ -GL479 complex crystallization, the reservoir solution was

composed by 27% PEG 20,000 and 0.1 M Tris-HCl pH 7.0, whereas the crystals of PPAR $\gamma$ -GL479 complex grew using the reservoir solution consisting of 0.8 M sodium citrate dehydrate and 0.1 M Hepes at pH 8.0. The crystals were cryoprotected by addition of 15% (v/v) of ethylene glycol in the same reservoir solution and flash cooled by immersion in liquid nitrogen prior to X-ray data collection. Diffraction data were collected at the MX-2 beamline, at LNLS (Brazilian Synchrotron Light Laboratory; Campinas, Brazil) and processed with XDS (Kabsch, 2010) and SCALA (Evans, 2011). The structures were determined by molecular replacement using PHASER (McCoy et al., 2007) and PDB entries 2P54 and 3SZ1 for PPAR $\alpha$  and PPAR $\gamma$ , respectively.

### 2.3. Refinement and structural analyses

Manual adjustments of the model to electron density were carried out using COOT (Emsley and Cowtan, 2004) and the structure refinement was performed with PHENIX (Adams et al., 2002). The geometry of the final models were checked with MOLPROBITY (Chen et al., 2010) and the interatomic contacts between protein-ligand were visualized by LIGPLOT program (Wallace et al., 1995). The protein alignment and analysis were carried with Pymol (The PyMOL Molecular Graphics System, Version 1.2r3pre, Schrödinger, LLC) and Chimera (Pettersen et al., 2004).

## 3. Results

### 3.1. Overall description of the X-ray structures of PPAR $\alpha$ and $\gamma$ in complex with GL479

Molecular structure of GL479 contains an acidic head group, an aromatic center and a hydrophobic tail connected by a three atoms linker (Fig. 1A). To understand the structural basis of PPAR $\alpha$ / $\gamma$  activation by this dual agonist and to gain further insights into its binding mode in each receptor, we co-crystallized GL479 with the human PPAR $\alpha$  and PPAR $\gamma$  ligand binding domains and determined the structures of both receptors bound to GL479. The

**Table 1**  
Statistics of crystallographic data and refinement.

	PPAR $\alpha$ :GL479	PPAR $\gamma$ :GL479
<i>Data collection</i>		
Wavelength Å/Beamline	1.459/LNLS-MX2	1.459/LNLS-MX2
Space group	<i>P</i> 4 <sub>1</sub> 2 <sub>1</sub> 2	<i>C</i> 2
Unit-cell parameters (Å, °)	64.53, 64.53, 124.4	88.49, 64.25, 118.78 90.0, 102.6, 90.0
Resolution range (Å)	44.78–2.30 (2.39–2.30)	37.85–1.77 (1.87–1.77)
Mean <i>I</i> / <i>r</i> ( <i>I</i> )	17.5 (3.0)	13.2 (2.0)
Multiplicity	5.3 (5.0)	3.2 (3.1)
Completeness	99.8 (98.7)	98.8 (97.9)
<i>R</i> <sub>merge</sub> <sup>a</sup> (%)	6.1 (49.8)	5.7 (62.5)
No. of molecules in asymmetric unit	1	2
No. of reflections	12,240 (1230)	62,608 (8968)
<i>Refinement</i>		
Resolution range (Å)	42.84–2.30	36.25–1.77
<i>R</i> <sub>factor</sub> / <i>R</i> <sub>free</sub>	21.88/26.64	16.94/20.82
<i>Average B factor</i>		
Protein	55.70	34.20
Ligand	60.7	43.34
<i>RMSD</i>		
Bond lengths (Å)	0.009	0.019
Bond angles (°)	1.10	1.75
Ramachandran plot (%)		
Most favoured regions	98.35	99.02
Disallowed regions	0	0

Statistics for the highest-resolution shell are shown in parentheses.

<sup>a</sup> *R*<sub>merge</sub> =  $\sum |I_j - \langle I \rangle| / \sum \langle I \rangle$ , where *I<sub>j</sub>* is the observed intensity of an individual reflection and  $\langle I \rangle$  is the average intensity of that reflection.



complexed PPAR $\alpha$ :GL479 and PPAR $\gamma$ :GL479 structures were solved to a resolution of 2.30 and 1.77 Å, respectively. The structure of the PPAR $\alpha$ :GL479 complex (Fig. 1B) belongs to the tetragonal space group  $P4_12_12$ , and contains a monomer (encompassing the amino acid residues from Lys204 to Met467) in the asymmetric unit. This corresponds to a  $V_M$  of 16.7 Å<sup>3</sup>/Da and a calculated solvent content of 41.17%. In addition to the protein monomer, the final model consists of one GL479 and 52 water molecules. The statistics of data collection, refinement and quality parameters of the final model are summarized in Table 1. The Ramachandran plot analysis showed that 98.35% of the residues are in the most favored and none in the disallowed regions.

The structure of the PPAR $\gamma$ :GL479 complex was solved in the monoclinic space group  $C2$ . Similar to the previously determined structures, the final model consists of two monomers in the asymmetric unit (encompassing the amino acid residues from Ala206 to Tyr477). The monomer designated as chain A represents the “active” conformation with displaced H12 (closed), and chain B in inactive conformation (H12 open) (Fig. 1C). The conformations adopted for both chains are almost identical, except for the

position of H12. The inactive conformation found in the chain B is caused by the crystal contacts with the chain A which prevent H12 to adopt the active conformation (Nolte et al., 1998). Furthermore, the final model contains two molecules of GL479, one in each chain, and 493 water molecules. The LBD structure has an overall fold practically identical to other of previously published PPAR LBDs complexes in the agonist-type conformation.

The structure is mainly formed by helices organized in a three-layered sandwich (13  $\alpha$ -helices and 3-stranded antiparallel  $\beta$ -sheet and unlike the other nuclear receptors, PPAR LBD contains an extra helix located between the first  $\beta$ -strand and H3 designated as H2'). The structures of PPAR $\alpha$ -LBD and PPAR $\gamma$ -LBD determined here are highly similar with an RMS (Root Mean Square) distance of 0.97 Å calculated for 242 common Ca positions of the chain A. Some regions showed a weak electron density, because of their high dynamic and disorder, and therefore were omitted from the final model. For PPAR $\alpha$ , disordered regions correspond to residues 230–237 and 255–266, whereas in the PPAR $\gamma$  structure the region between residues 262–275 is disordered. The later region of the PPAR $\gamma$  and the correspondent region of PPAR $\alpha$  consist of the

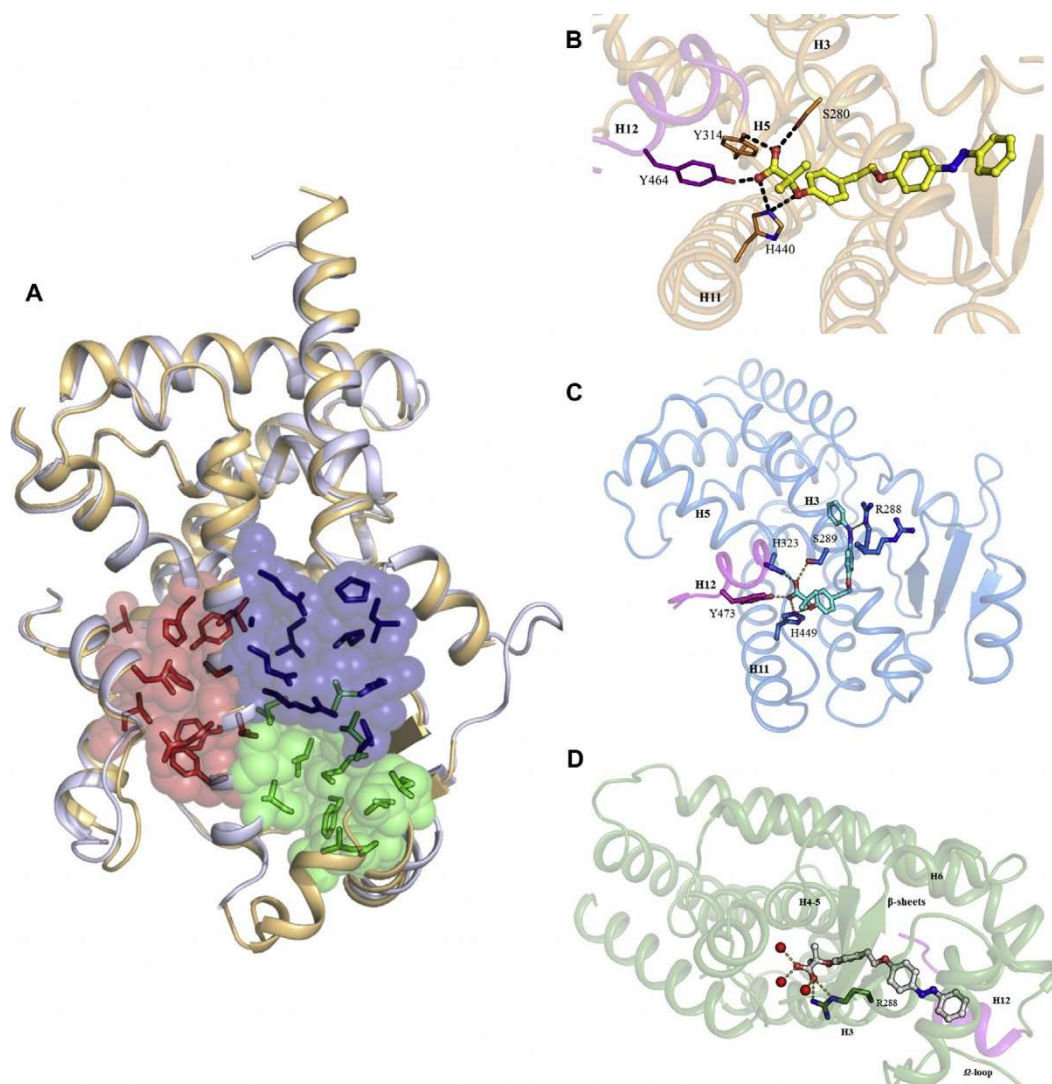


**Fig. 2.** Structural characterization of GL479. (A) Overall structure of LBDs PPAR $\alpha$  (light orange) and PPAR $\gamma$  (blue white) displaying the three arms of the LBP: the arm I (red), the arm II (blue) and the arm III (green). (B) Details of interactions between PPAR $\alpha$  and GL479. The GL479 head carboxylic group makes interactions with the polar side chains, including Y464, which results in the PPAR $\alpha$  LBD canonical active conformations of helix 12. (C) Active monomer and (D) inactive B-subunit of PPAR $\gamma$  complexed with GL479. The polar amino acid residues that interact with the ligands are labeled and shown as sticks. H12 is painted in purple.



**Fig. 3.** Overlap of GL479 in complexes with PPAR $\alpha$  and PPAR $\gamma$ . GL479 occupied the ligand-binding pocket of PPAR $\alpha$  (red) and PPAR $\gamma$  (gray) in two distinct conformations. The acid group adopted essentially the same configuration in both conformations. However, its hydrophobic tail was in two completely configurations. In the first binding mode, exemplified by PPAR $\alpha$  structure, the hydrophobic tail bends upward into the upper arm of the Y-shaped pocket (arm II). In the second binding mode (inside of PPAR $\gamma$  LBP), the hydrophobic tail of GL479 bends downward into the arm III at the bottom of the LBP. Ligands are shown as sticks and balls.

$\Omega$ -loop, located between H2' and H3. The  $\Omega$ -loop is highly flexible in nuclear receptors and a number of studies suggest that this region is responsible for the entrance of ligands inside the PPAR LBP (Liberato et al., 2012; Lu et al., 2006; Puhl et al., 2012; Zoete et al., 2007) and is highly mobile (Kuwabara et al., 2012; Nolte et al., 1998; Pochetti et al., 2007).

### 3.2. Different binding modes of GL479 for PPAR $\alpha$ and PPAR $\gamma$ - both dependent of H12

The ligand molecules were not included in the protein model until the final stages of refinement. In order to reduce the effects of model bias, the omit maps of the ligand pockets were calculated for both structures and they revealed clear electronic densities for the bound ligands, thus enabling the unambiguously positioning of them into the LBP of each receptor (Supplementary material).

The PPARs have Y-shaped ligand-binding cavity, which extends from the C-terminal helix to the  $\beta$ -sheet, divided into three arms that display significant homology (60–70%) between the subtypes (Xu et al., 2001). The left arm of the Y (arm I) is composed of a mix of hydrophobic and polar residues, including two residues from the AF-2 helix, whereas, the right and lower arms (arms II and III, respectively) are mainly composed by hydrophobic residues (Fig. 2A).

GL479 occupies about 30% of the total volume of the PPAR $\alpha$  and PPAR $\gamma$  Y-shaped ligand-binding cavity, which extends from the C-terminal helix to the  $\beta$ -sheet, lying between helices H3 and H6. In both PPAR subtypes structures, GL479 is stabilized through a combination of hydrogen bonds and hydrophobic interactions. The region occupied by GL479 inside of the PPAR $\alpha$  LBP fits U-shaped conformation and adjoin the H2', H3, H7, H10/11, H12, and  $\beta$ -strand 2 and 3, so occupying the region of arms I and III. Such ligand arrangement inside of protein pocket allows the

formation of four hydrogen bonds of its carboxylic group with the residues S280 (H3), Y314 (H5), H440 (H11) and Y464 (H12), including one bond with the first phenoxy group S280 (H3). In addition to the hydrogen bonds, many hydrophobic interactions are formed with ligand tail assisting in the stabilization of the GL479. These contacts are formed by the residues L247, F273, C276, Q277, T279, F318, L321, V332, I354, M355 and L460. In addition, there are several polar interactions between the GL479 and PPAR $\alpha$ -LBD which are shown in Fig. 2B

Strikingly, for PPAR $\gamma$  complex, the ligand adopted a conformation and occupation very different from that observed for PPAR $\alpha$  and for the most full agonists in a U-shaped conformation (Bruning et al., 2007; Nolte et al., 1998). Similarly to PPAR $\alpha$ :GL479, PPAR $\gamma$ :GL479 complex (chain A), also presents the typical pattern of hydrogen bonds cluster, located in the arm I of its LBP, involving the residues S289 (H3), H323 (H6), H449 (H11) and Y473 (H12) (Fig. 2C). The conservation of the network of hydrogen bonds and H12 direct stabilization suggests that it should be critical for GL479-mediated activation of both receptors.

However, the set of hydrophobic interactions made by the nonpolar ligand tail differs in each context. The most residues that form the nonpolar contacts with GL479 occupy the arm II of PPAR $\gamma$  LBP, encompassing F226, R288, A292, M329, L330 and M364. This forces the ligand to adopt an S-shaped conformation (Li et al., 2008). Additionally, the diazene group of the ligand tail forms a weak hydrogen bond with R288, also located in the ligand pocket arm II (Fig. 2C). This interaction appears to be essential to the partial agonism of GL479 and it has been poorly explored in the discovery of new partial agonists. In other PPAR $\chi$  structures, where a hydrogen bond between ligand and R288 is also found, this correlates with a low receptor activation elicited by the ligands (Casimiro-Garcia et al., 2013; Connors et al., 2009). However, contrasting with PPAR $\gamma$ :GL479 complex, these others ligands do not present direct interaction with the receptor H12. Many regions of the PPARs structures already have been associated with the partial activation, but the importance of the interaction between the ligand and R288 and its effect on partial agonism has not been widely recognized as so far. Nevertheless, when this interaction is observed, the partial agonism is predominant, suggesting that this interaction could be explored further in the search for new partial PPAR $\gamma$  agonists.

In the PPAR $\gamma$  LBD chain B, the ligand is also held in place by several interactions. There are five hydrogen bonds, two are between the polar head of the ligand and R288 side chain and the other three are formed with waters molecules. In addition, the ligand is also stabilized by the hydrophobic contacts (Fig. 2D). However, since this chain is forced into inactive conformation by the crystal packaging, physiological relevance of these interactions is not clear.

Comparisons between PPAR $\alpha$ / $\gamma$ :GL479 complexes showed that despite the dissimilarities, both structures include a hydrogen bond between the residues located in the AF2-helix, which compels it to adopt the active conformation, i.e., the “closed state”. The divergence of GL479 occupancy in each receptor could be better visualized in the Fig. 3.

### 3.3. PPAR LBP occupancy versus full/partial agonism

The two X-ray complex structures nicely allow to rationalize the functional patterns observed in the transactivation assays, describing GL479 as a full agonist for PPAR $\alpha$  and as a partial agonist for PPAR $\gamma$ . Based on previous studies, it has been suggested that PPAR full agonists generally have direct interactions with residues of helix 12, primarily through the formation of a hydrogen bond between the carboxylic group of ligands and tyrosine residues located in the AF-2 region. Differently, partial agonists

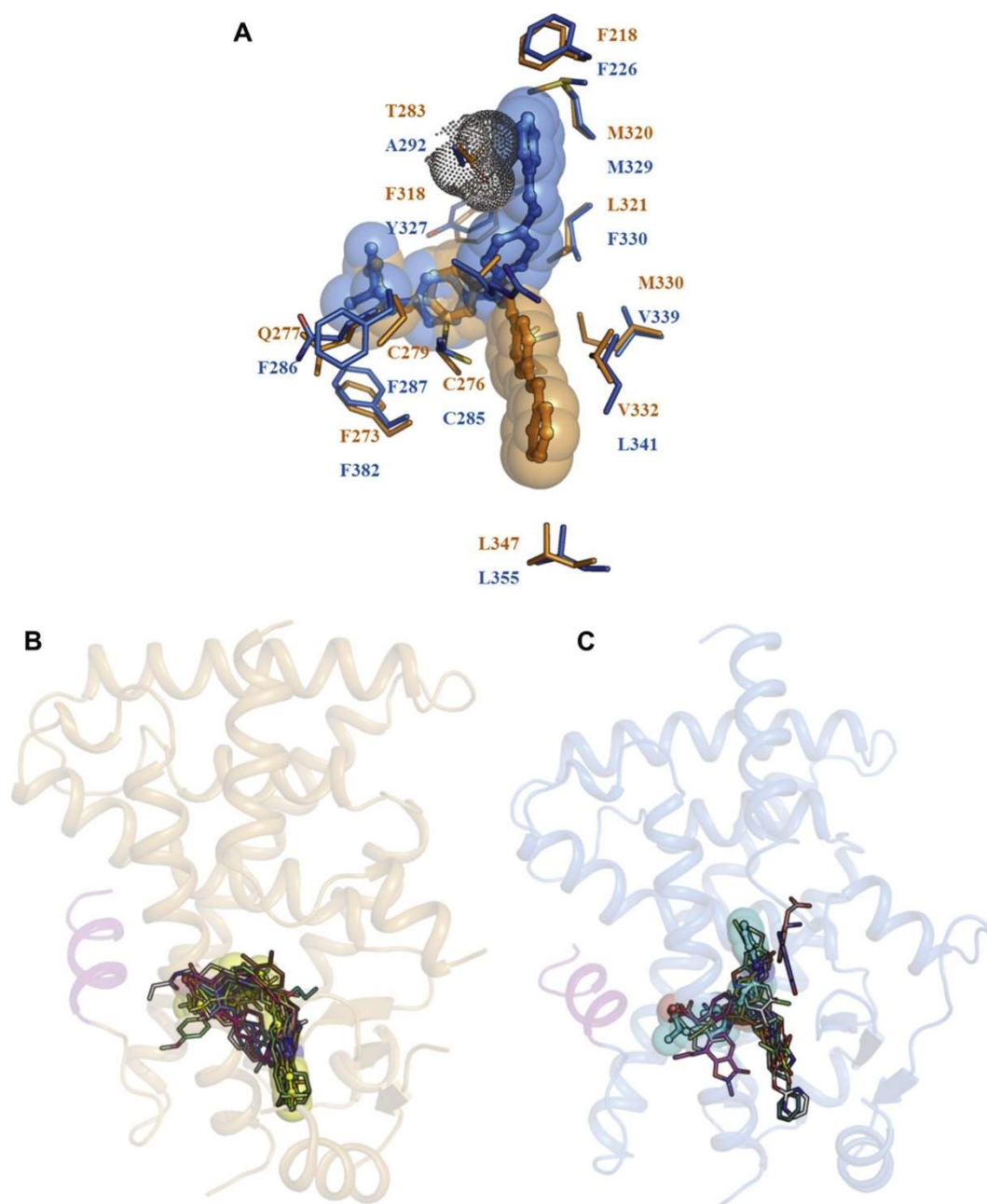


**Fig. 4.** Structural comparisons between the crystallographic models of PPAR $\alpha$  and PPAR $\gamma$  LBD. (A) Superposition of the GL479 ligand bound PPAR $\alpha$  (orange) and PPAR $\gamma$  (blue). Only residues that are involved in nonpolar interactions are shown. The position of PPAR $\gamma$  A292 is replaced by PPAR $\alpha$  T273, and the later bigger side chain (dots) impairs the accommodation of GL479 rings in the same region of LBP. (B) All the reported crystal structures of PPAR $\alpha$ :agonists complex with the ligands in the U-shaped inside of receptor pocket which coincide with GL479 (stick and ball yellow) occupation. (C) Some PPAR $\gamma$  agonists were observed occupying S-pocket in agreement with GL479 position (stick ball cyan).

stabilize other regions of the LBP, without direct contact with the helix 12 [Bruning et al., 2007]. The variations observed in the receptor apo, full-agonist-, and partial-agonist-bound activities leads to the premise that it is controlled by ligand binding modes and mainly by H12 dynamics. The studies with fluorescence labeled H12 [Kallenberger et al., 2003] demonstrated that the degree of H12 helix stabilization is proportional to the degree of agonism and transcriptional output for full agonists.

To comprehend potential molecular determinants of differentiated binding mode and an activation pattern of two subtypes, we carried out a detailed comparison of both three-dimensional structures by their superposition and alignment of their backbones (R.M.S. of 0.814). Among residues involved in the ligand tail

stabilization only the position of PPAR $\alpha$  T273 is replaced by PPAR $\gamma$  A292. The side chain of PPAR $\alpha$  T273 occupies more space and impairs the accommodation of GL479 rings in the region described for PPAR $\gamma$  complex formation (Fig. 4A). This substitution could also be the reason why it has not been yet reported X-ray structures with ligand binding in the region of arm II. PPAR $\alpha$  agonists always bind in the ligand binding pocket in an U-conformation as can be observed in Fig. 4B. On the contrary, PPAR $\gamma$  agonists were observed occupying S-pocket (Fig. 4C), and this binding mode might play an important role in mediating ligand-dependent conformational changes that facilitate recruitment of coregulator proteins, such as NCoR [Li et al., 2008], which are consistent with lower transcriptional activity and partial



agonism pattern observed for PPAR $\gamma$ . However, the preference of GL479 for PPAR $\gamma$  arm II may be due to hydrogen bond formation between side chain of PPAR $\gamma$  R288 and nitrogen atoms of ligand tail in addition to the increased number of apolar interactions. There are some residues substitutions in PPAR $\gamma$  as compared to PPAR $\alpha$  receptor that are involved in the hydrophobic interactions with the ligand (PPAR $\alpha$  M330/PPAR $\gamma$  V339 and PPAR $\alpha$  C275/PPAR $\gamma$  G284). Thus, the same interactions cannot be formed in PPAR $\gamma$  LBP arm III.

GL479 and two other compounds, all synthesized and described by Giampietro et al. (2012), share the same functional features, i.e. full agonist for the PPAR $\alpha$  agonist and partial agonist for PPAR $\gamma$ . The unique difference among these compounds structure is the length of the linker between the aromatic lipophilic tail and the center (one, two or three carbons). Although only the studies with GL479 (linker with two carbons) have resulted in the crystal structures of complexes, we believe that this minor variation on the link size is not enough to change the current position of the ligand in each receptor structure, since the addition or deletion of this carbon atoms would not cause steric hindrance with residues of the PPARs active sites.

B-factors analysis of our structures showed that GL479 stabilizes differently several regions of the PPAR $\alpha$  and PPAR $\gamma$  structures. The GL479 produces a stronger stabilization of the loop that comprises H11 and H12 of PPAR $\gamma$  (Fig. 5A), while the region close to X-loop is better stabilized in PPAR $\alpha$  complex (Fig. 5B). This greater stability of the region adjacent to O-loop for PPAR $\alpha$  receptor might cause conformational changes that produce a decrease in the helix 12 mobility leading to stabilization of its the interactions with coactivators (Bernardes et al., 2013).

In fact, these data agree with the hypothesis that the direct interaction with H12 is not the only mediator of transcriptional responses (Bruning et al., 2007), but additional stabilization of certain regions of receptor structure provided by interaction with ligand hydrophobic tail could indirectly influence the H12 dynamic. Furthermore, a polar interaction with  $\gamma$ R288 may be also related with partial agonism profile of ligands. In other words, the transcriptional activity observed for a ligand is dictated by its receptor binding mode, and it is not only restricted to the presence or absence of direct interactions with H12. PPARs ligand-binding domains have large volumes and display high intrinsic mobility, which allow them to assume a continuum of conformations, adopting multiple activated states and facilitating interactions with different coregulators (Li et al., 2008; Xu et al., 2002).

We propose that the active conformation of both PPAR subtypes is accessible due to hydrogen bonds network, but the ligand configuration adopted for PPAR $\gamma$  receptor is not sufficient to stabilize the protein structure like in a U-shaped full agonists mode.

Consequently, the coactivator recruitment becomes weaker, which restricts the receptor activity. Nevertheless, since the ligand fills in the arm III of the ligand-binding pocket, this shifts the equilibrium toward the active configuration of the receptor via indirect AF-2 stabilization.

#### 4. Discussion

The important role of PPARs in metabolic diseases such as T2DM and dyslipidemia has been well established by numerous functional studies (Berger and Moller, 2002; Forman et al., 1995; Kota et al., 2005; Lehmann et al., 1995; Nolte et al., 1998). It is also known that the TZDs drugs rosiglitazone and pioglitazone improve insulin resistance by PPAR $\gamma$  activation, and that PPAR $\alpha$  activation by fibrates induces a decrease in circulating lipid levels. Despite the fact that many dual PPAR agonists been synthesized, a drug that could have both therapeutic effects is not available yet because of serious side-effects already observed in both preclinical and clinical studies. However, balanced dual PPAR $\alpha/\gamma$  agonists could potentially benefit patients with diabetes and metabolic disorder (Cavender and Lincoff, 2010). Thus, it is of considerable importance to identify, describe and understand the action mechanism of novel dual PPAR- $\alpha/\gamma$  agonists. To date the mode of receptor binding has been structurally characterized for only a few dual PPAR $\alpha/\gamma$  agonists (B  nardeau et al., 2009; Cronet et al., 2001; Grether et al., 2009; Xu et al., 2001), and this information about ligands occupation in the binding pocket is crucially important. In all cases described, the ligand adopts the identical active conformation, occupying the arm I and III of the ligand binding pocket and has a similar mode of binding for both PPARs (Fig. 6). The GL479 in complex with the PPAR $\alpha$  stabilizes the region occupied by others full agonists such as AZ242 (Cronet et al., 2001), APHM13 (Kuwabara et al., 2012) and oxybenzylglycine derivatives (Li et al., 2010) mainly decreasing mobility of the helices H3, H5, H7, H11 and H12 of the LBD. In these complexes, the acidic head of the ligand buried the arm I forms hydrogen bonds network with the polar residues S280, Y314, Y464 and H440, whereas the hydrophobic part of the ligand occupies the arm II and is stabilized mainly by extensive van der Waals interactions. It is assumed that

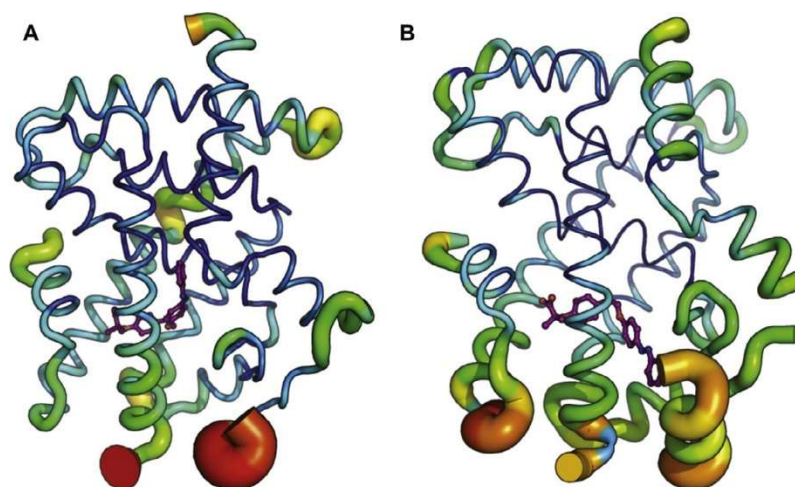


**Fig. 5.** GL479-induced stabilization of different regions of PPAR $\alpha$  and  $\gamma$ . The structures are colored and represented according to their *B*-factors. (A) PPAR $\gamma$ -LBD and (B) PPAR $\alpha$ -LBD.



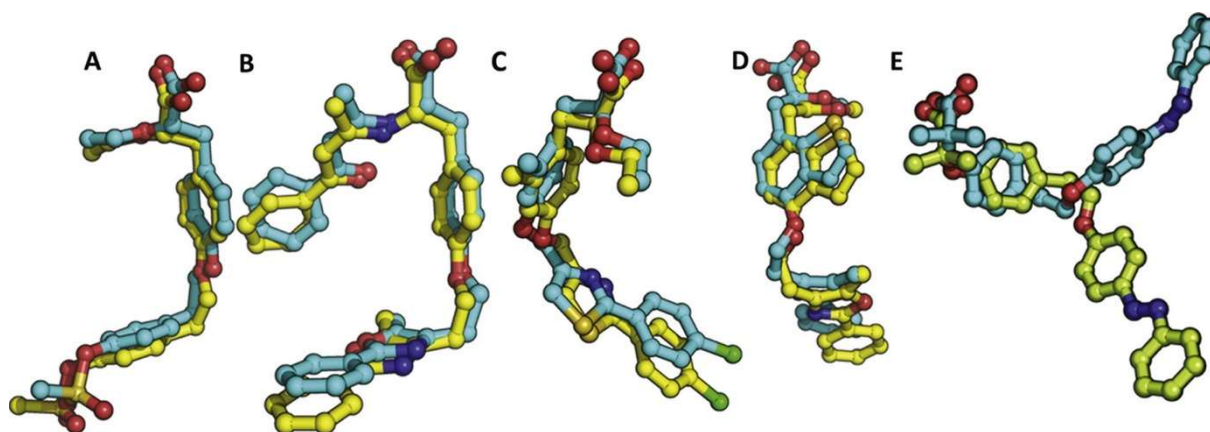


**Fig. 6.** Superimposed PPAR $\alpha$  and PPAR $\gamma$  active monomers crystallized with different dual agonists. Only GL479 (*E*) displayed a divergent binding mode for  $\alpha$  and  $\gamma$  subtypes.

the full agonist activity is associated that the later mode of binding observed in all known structures of the PPAR $\alpha$ . As a general rule the potent PPAR $\alpha$  ligands which have high affinity to the receptor make direct interactions with H12 (Grether et al., 2009; Kuwabara et al., 2012; Li et al., 2010; Oon Han et al., 2007). Surprisingly, the GL479 binds to PPAR $\gamma$  in a singular mode of binding, different from all currently available structures of the receptor:ligand complexes. As a rule, the PPARs partial agonists do not interact with the tyrosine residue of H12 in active conformation (Bruning et al., 2007; Xu et al., 2001). Nevertheless, in our structure we can clearly observe the interaction between GL479 and Tyr473 (H12) of PPAR $\gamma$ . For the first time, we found a partial agonist interacting H12. Another important aspect of this complex is that the GL479 adopts a particular conformation in the active site, extending through the arms I and arm II of LBP, differently of the occupation described for full agonists. This mode of ligand binding has not been described to date for any available PPARs complexes and might indicate that simultaneous occupation of arms I and III ensures the most active conformation of the receptor.

We have provided a detailed structural analysis of a PPAR $\alpha/\gamma$  dual agonist mode of binding to the receptors. Two particular structural features distinguish the binding of this amphipathic ligand to PPAR $\alpha/\gamma$  subtypes. First, the carboxylic acid head makes an intricate series of hydrogen bonds with the receptor, which are the chiefly responsible for ligand:protein interactions and for

inducing the active conformation of H12. However, the receptor activation pattern is mediated by the ligand tail conformation, demonstrating that the stabilization of specific regions of the LBDs could ensure the mode of receptor activation.

Importantly, the ligands with attenuated PPAR $\gamma$  activation may be promising, since the clinical use of PPAR $\gamma$  agonists has been complicated by weight gain, fluid retention and arising in cardiovascular events that is often encountered (Calkin and Thomas, 2008). On the other hand, full agonism of PPAR $\alpha$  has been largely well tolerated. If novel functional studies confirm the dual PPAR $\alpha/\gamma$  agonist nature of GL479 and the theoretical benefit of this ligand class, GL479 may become a promising alternative of the therapy currently employed in the treatment of dyslipidemia and dysglycemia in patients with type 2 diabetes.

#### Author contributions

JCS, AB, LG, AA BF designed experiments; JCS performed the experiments; JCS and AB analyzed data and wrote the manuscript; RA and IP conceived and supervised the study and made manuscript revisions.

#### Acknowledgments

This work is supported by Fundação de Amparo à Pesquisa do Estado de São Paulo (FAPESP) via grants 2009/14333-6 (JCS), 2007/58443-4 (AB) and 2008/56255-9 (IP), Conselho Nacional de Desenvolvimento Científico e Tecnológico (CNPq) (IP) and Italian MIUR (RA). We are also grateful to the Brazilian National Synchrotron Light Laboratory (LNLS, Campinas, Brazil) for the use of the MX-2 beam line.

#### Appendix A. Supplementary data

Supplementary data associated with this article can be found, in the online version, at <http://dx.doi.org/10.1016/j.jsb.2015.07.006>.

#### References

- Adams, P.D., Grosse-Kunstleve, R.W., Hung, L.W., Ioerger, T.R., McCoy, A.J., Moriarty, N.W., Read, R.J., Sacchettini, J.C., Sauter, N.K., Terwilliger, T.C., 2002. PHENIX: building new software for automated crystallographic structure determination. *Acta Crystallogr. D Biol. Crystallogr.* 58, 1948–1954.
- Argmann, C.A., Cock, T.A., Auwerx, J., 2005. Peroxisome Proliferator-Activated Receptor gamma: the more the merrier? *Eur. J. Clin. Invest.* 35, 82–92, discussion 80.
- Auwerx, J., 1999. PPARgamma, the ultimate thrifty gene. *Diabetologia* 42, 1033–1049.
- Auwerx, J., Cock, T.A., Knouff, C., 2003. PPAR-gamma: a thrifty transcription factor. *Nucl. Recept. Signal.* 1, e006.
- Barter, P.J., Rye, K.A., 2008. Is there a role for fibrates in the management of dyslipidemia in the metabolic syndrome? *Arterioscler. Thromb. Vasc. Biol.* 28, 39–46.
- Berger, J., Moller, D.E., 2002. The mechanisms of action of PPARs. *Annu. Rev. Med.* 53, 409–435.
- Bernardes, A., Souza, P.C., Muniz, J.R., Ricci, C.G., Ayers, S.D., Parekh, N.M., Godoy, A.S., Trivella, D.B., Reinach, P., Webb, P., Skaf, M.S., Polikarpov, I., 2013. Molecular mechanism of Peroxisome Proliferator-Activated Receptor  $\alpha$  activation by WY14643: a new mode of ligand recognition and receptor stabilization. *J. Mol. Biol.*
- Bruning, J.B., Chalmers, M.J., Prasad, S., Busby, S.A., Kamenecka, T.M., He, Y., Nettles, K.W., Griffin, P.R., 2007. Partial agonists activate PPARgamma using a helix 12 independent mechanism. *Structure* 15, 1258–1271.
- Bénardeau, A., Benz, J., Binggeli, A., Blum, D., Boehringer, M., Grether, U., Hilpert, H., Kuhn, B., Märki, H.P., Meyer, M., Püntener, K., Raab, S., Ruf, A., Schlatter, D., Mohr, P., 2009. Aleglitazar, a new, potent, and balanced dual PPARalpha/gamma agonist for the treatment of type II diabetes. *Bioorg. Med. Chem. Lett.* 19, 2468–2473.
- Calkin, A.C., Thomas, M.C., 2008. PPAR agonists and cardiovascular disease in diabetes. *PPAR Res.* 2008, 245410.
- Casimiro-Garcia, A., Heemstra, R.J., Bigge, C.F., Chen, J., Ciske, F.A., Davis, J.A., Ellis, T., Esmaeil, N., Flynn, D., Han, S., Jalaie, M., Ohren, J.F., Powell, N.A., 2013. Design, synthesis, and evaluation of imidazo[4,5-c]pyridin-4-one derivatives with dual activity at angiotensin II type 1 receptor and peroxisome proliferator-activated receptor-C. *Bioorg. Med. Chem. Lett.* 23, 767–772.
- Cavender, M.A., Lincoff, A.M., 2010. Therapeutic potential of aleglitazar, a new dual PPAR- $\alpha/\gamma$  agonist: implications for cardiovascular disease in patients with diabetes mellitus. *Am. J. Cardiovasc. Drugs* 10, 209–216.

- Chen, V.B., Arendall, W.B., Headd, J.J., Keedy, D.A., Immormino, R.M., Kapral, G.J., Murray, L.W., Richardson, J.S., Richardson, D.C., 2010. MolProbity: all-atom structure validation for macromolecular crystallography. *Acta Crystallogr. D Biol. Crystallogr.* 66, 12–21.
- Choi, J.H., Banks, A.S., Estall, J.L., Kajimura, S., Boström, P., Laznik, D., Ruas, J.L., Chalmers, M.J., Kamenecka, T.M., Blüher, M., Griffin, P.R., Spiegelman, B.M., 2010. Anti-diabetic drugs inhibit obesity-linked phosphorylation of PPARgamma by Cdk5. *Nature* 466, 451–456.
- Cock, T.A., Houten, S.M., Auwerx, J., 2004. Peroxisome proliferator-activated receptor-gamma: too much of a good thing causes harm. *EMBO Rep.* 5, 142–147.
- Connors, R.V., Wang, Z., Harrison, M., Zhang, A., Wanska, M., Hiscock, S., Fox, B., Dore, M., Labelle, M., Sudom, A., Johnstone, S., Liu, J., Walker, N.P., Chai, A., Siegler, K., Li, Y., Coward, P., 2009. Identification of a PPARdelta agonist with partial agonistic activity on PPARgamma. *Bioorg. Med. Chem. Lett.* 19, 3550–3554.
- Cronet, P., Petersen, J.F., Folmer, R., Blomberg, N., Sjöblom, K., Karlsson, U., Lindstedt, E.L., Bamberg, K., 2001. Structure of the PPARalpha and -gamma ligand binding domain in complex with AZ 242; ligand selectivity and agonist activation in the PPAR family. *Structure* 9, 699–706.
- Eckel, R.H., Grundy, S.M., Zimmet, P.Z., 2005. The metabolic syndrome. *Lancet* 365, 1415–1428.
- Emsley, P., Cowtan, K., 2004. Coot: model-building tools for molecular graphics. *Acta Crystallogr. D Biol. Crystallogr.* 60, 2126–2132.
- Evans, P.R., 2011. An introduction to data reduction: space-group determination, scaling and intensity statistics. *Acta Crystallogr. D Biol. Crystallogr.* 67, 282–292.
- Fiévet, C., Fruchart, J.C., Staels, B., 2006. PPARalpha and PPARgamma dual agonists for the treatment of type 2 diabetes and the metabolic syndrome. *Curr. Opin. Pharmacol.* 6, 606–614.
- Forman, B.M., Chen, J., Evans, R.M., 1997. Hypolipidemic drugs, polyunsaturated fatty acids, and eicosanoids are ligands for peroxisome proliferator-activated receptors alpha and delta. *Proc. Natl. Acad. Sci. U.S.A.* 94, 4312–4317.
- Forman, B.M., Tontonoz, P., Chen, J., Brun, R.P., Spiegelman, B.M., Evans, R.M., 1995. 15-Deoxy-delta 12, 14-prostaglandin J2 is a ligand for the adipocyte determination factor PPAR gamma. *Cell* 83, 803–812.
- Giampietro, L., D'Angelo, A., Giancristofaro, A., Ammazalorso, A., De Filippis, B., Fantacuzzi, M., Linciano, P., Maccallini, C., Amoroso, R., 2012. Synthesis and structure-activity relationships of fibrate-based analogues inside PPARs. *Bioorg. Med. Chem. Lett.* 22, 7662–7666.
- Grether, U., Bénardeau, A., Benz, J., Binggeli, A., Blum, D., Hilpert, H., Kuhn, B., Märki, H.P., Meyer, M., Mohr, P., Püntener, K., Raab, S., Ruf, A., Schlatter, D., 2009. Design and biological evaluation of novel, balanced dual PPARalpha/gamma agonists. *ChemMedChem* 4, 951–956.
- Harmon, G.S., Lam, M.T., Glass, C.K., 2011. PPARs and lipid ligands in inflammation and metabolism. *Chem. Rev.* 111, 6321–6340.
- Henke, B.R., Blanchard, S.G., Brackeen, M.F., Brown, K.K., Cobb, J.E., Collins, J.L., Harrington, W.W., Hashim, M.A., Hull-Ryde, E.A., Kaldor, I., Kliewer, S.A., Lake, D.H., Leesnitzer, L.M., Lehmann, J.M., Lenhard, J.M., Orband-Miller, L.A., Miller, J.F., Mook, R.A., Noble, S.A., Oliver, W., Parks, D.J., Plunket, K.D., Szewczyk, J.R., Willson, T.M., 1998. N-(2-Benzoylphenyl)-L-tyrosine PPARgamma agonists. 1. Discovery of a novel series of potent antihyperglycemic and antihyperlipidemic agents. *J. Med. Chem.* 41, 5020–5036.
- Inzucchi, S.E., Bergenstal, R.M., Buse, J.B., Diamant, M., Ferrannini, E., Nauck, M., Peters, A.L., Tsapas, A., Wender, R., Matthews, D.R., 2015. Management of hyperglycemia in type 2 diabetes, 2015: a patient-centered approach: update to a position statement of the American Diabetes Association and the European Association for the Study of Diabetes. *Diabetes Care* 38, 140–149.
- Kabsch, W., 2010. XDS. *Acta Crystallogr. D Biol. Crystallogr.* 66, 125–132.
- Kallenberger, B.C., Love, J.D., Chatterjee, V.K., Schwabe, J.W., 2003. A dynamic mechanism of nuclear receptor activation and its perturbation in a human disease. *Nat. Struct. Biol.* 10, 136–140.
- Kota, B.P., Huang, T.H., Roufogalis, B.D., 2005. An overview on biological mechanisms of PPARs. *Pharmacol. Res.* 51, 85–94.
- Kuwabara, N., Oyama, T., Tomioka, D., Ohashi, M., Yanagisawa, J., Shimizu, T., Miyachi, H., 2012. Peroxisome proliferator-activated receptors (PPARs) have multiple binding points that accommodate ligands in various conformations: phenylpropanoic acid-type PPAR ligands bind to PPAR in different conformations, depending on the subtype. *J. Med. Chem.* 55, 893–902.
- Lehmann, J.M., Moore, L.B., Smith-Oliver, T.A., Wilkison, W.O., Willson, T.M., Kliewer, S.A., 1995. An antidiabetic thiazolidinedione is a high affinity ligand for peroxisome proliferator-activated receptor gamma (PPAR gamma). *J. Biol. Chem.* 270, 12953–12956.
- Levin, D., Bell, S., Sund, R., Hartikainen, S.A., Tuomilehto, J., Pukkala, E., Keskimäki, I., Badrick, E., Renahan, A.G., Buchan, I.E., Bowker, S.L., Minhas-Sandhu, J.K., Zafari, Z., Marra, C., Johnson, J.A., Stricker, B.H., Uitterlinden, A.G., Hofman, A., Ruiter, R., de Keyser, C.E., MacDonald, T.M., Wild, S.H., McKeigue, P.M., Colhoun, H.M., Scottish Diabetes Research Network Epidemiology Group, Diabetes and Cancer Research Consortium, 2015. Pioglitazone and bladder cancer risk: a multipopulation pooled, cumulative exposure analysis. *Diabetologia* 58, 493–504.
- Li, J., Kennedy, L.J., Shi, Y., Tao, S., Ye, X.Y., Chen, S.Y., Wang, Y., Hernández, A.S., Wang, W., Devasthale, P.V., Chen, S., Lai, Z., Zhang, H., Wu, S., Smirk, R.A., Bolton, S.A., Ryono, D.E., Lim, N.K., Chen, B.C., Locke, K.T., O'Malley, K.M., Zhang, L., Srivastava, R.A., Miao, B., Meyers, D.S., Monshizadegan, H., Search, D., Grimm, D., Zhang, R., Harrity, T., Kunselman, L.K., Cap, M., Kadiyala, P., Hosagrahara, V., Xu, C., Li, Y.X., Muckelbauer, J.K., Chang, C., An, Y., Krystek, S.R., Blannar, M.A., Zahler, R., Mukherjee, R., Cheng, P.T., Tino, J.A., 2010. Discovery of an oxybenzylglycine based peroxisome proliferator activated receptor alpha selective agonist 2-((3-((2-(4-chlorophenyl)-5-methoxazol-4-yl)methoxy)benzyl)(methoxycarbonyl)amino)acetic acid (BMS-687453). *J. Med. Chem.* 53, 2854–2864.
- Li, Y., Wang, Z., Furukawa, N., Escaron, P., Weizmann, J., Lee, G., Lindstrom, M., Liu, J., Liu, X., Xu, H., Plotnikova, O., Prasad, V., Walker, N., Learned, R.M., Chen, J.L., 2008. T2384, a novel antidiabetic agent with unique peroxisome proliferator-activated receptor gamma binding properties. *J. Biol. Chem.* 283, 9168–9176.
- Liberato, M.V., Nascimento, A.S., Ayers, S.D., Lin, J.Z., Cvorov, A., Silveira, R.L., Martínez, L., Souza, P.C., Saidenberg, D., Deng, T., Amato, A.A., Togashi, M., Hsueh, W.A., Phillips, K., Palma, M.S., Neves, F.A., Skaf, M.S., Webb, P., Polikarpov, I., 2012. Medium chain fatty acids are selective peroxisome proliferator activated receptor (PPAR)  $\gamma$  activators and pan-PPAR partial agonists. *PLoS ONE* 7, e36297.
- Liu, C., Feng, T., Zhu, N., Liu, P., Han, X., Chen, M., Wang, X., Li, N., Li, Y., Xu, Y., Si, S., 2015. Identification of a novel selective agonist of PPAR $\gamma$  with no promotion of adipogenesis and less inhibition of osteoblastogenesis. *Sci. Rep.* 5, 9530.
- Lu, L.L., Huang, C.F., Peng, Y.H., Lin, Y.T., Hsieh, H.P., Chen, C.T., Lien, T.W., Lee, H.J., Mahindroo, N., Prakash, E., Yueh, A., Chen, H.Y., Goparaju, C.M., Chen, X., Liao, C.C., Chao, Y.S., Hsu, J.T., Wu, S.Y., 2006. Structure-based drug design of a novel family of PPARgamma partial agonists: virtual screening, X-ray crystallography, and in vitro/in vivo biological activities. *J. Med. Chem.* 49, 2703–2712.
- Mandart, S., Müller, M., Kersten, S., 2004. Peroxisome proliferator-activated receptor alpha target genes. *Cell. Mol. Life Sci.* 61, 393–416.
- McCoy, A.J., Grosse-Kunstleve, R.W., Adams, P.D., Winn, M.D., Storoni, L.C., Read, R.J., 2007. Phaser crystallographic software. *J. Appl. Crystallogr.* 40, 658–674.
- Michalik, L., Auwerx, J., Berger, J.P., Chatterjee, V.K., Glass, C.K., Gonzalez, F.J., Grimaldi, P.A., Kadowaki, T., Lazar, M.A., O'Rahilly, S., Palmer, C.N., Plutzky, J., Reddy, J.K., Spiegelman, B.M., Staels, B., Wahli, W., 2006. International Union of Pharmacology. LXI. Peroxisome proliferator-activated receptors. *Pharmacol. Rev.* 58, 726–741.
- Nathan, D.M., Buse, J.B., Davidson, M.B., Ferrannini, E., Holman, R.R., Sherwin, R., Zinman, B., Association, A.D., Diabetes, E.A.F.S.O., 2009. Medical management of hyperglycemia in type 2 diabetes: a consensus algorithm for the initiation and adjustment of therapy: a consensus statement of the American Diabetes Association and the European Association for the Study of Diabetes. *Diabetes Care* 32, 193–203.
- Nolte, R.T., Wisely, G.B., Westin, S., Cobb, J.E., Lambert, M.H., Kurokawa, R., Rosenfeld, M.G., Willson, T.M., Glass, C.K., Milburn, M.V., 1998. Ligand binding and co-activator assembly of the peroxisome proliferator-activated receptor- gamma. *Nature* 395, 137–143.
- Oon Han, H., Kim, S.H., Kim, K.H., Hur, G.C., Joo Yim, H., Chung, H.K., Ho Woo, S., Dong Koo, K., Lee, C.S., Sung Koh, J., Kim, G.T., 2007. Design and synthesis of oxime ethers of alpha-acyl-beta-phenylpropanoic acids as PPAR dual agonists. *Bioorg. Med. Chem. Lett.* 17, 937–941.
- Pettersen, E.F., Goddard, T.D., Huang, C.C., Couch, G.S., Greenblatt, D.M., Meng, E.C., Ferrin, T.E., 2004. UCSF Chimera – a visualization system for exploratory research and analysis. *J. Comput. Chem.* 25, 1605–1612.
- Pochetti, G., Godio, C., Mitro, N., Caruso, D., Galmozzi, A., Scurati, S., Loiodice, F., Fracchiolla, G., Tortorella, P., Laghezza, A., Lavecchia, A., Novellino, E., Mazza, F., Crestani, M., 2007. Insights into the mechanism of partial agonism: crystal structures of the peroxisome proliferator-activated receptor gamma ligand-binding domain in the complex with two enantiomeric ligands. *J. Biol. Chem.* 282, 17314–17324.
- Puhl, A.C., Bernardes, A., Silveira, R.L., Yuan, J., Campos, J.L., Saidenberg, D.M., Palma, M.S., Cvorov, A., Ayers, S.D., Webb, P., Reinach, P.S., Skaf, M.S., Polikarpov, I., 2012. Mode of peroxisome proliferator-activated receptor C activation by luteolin. *Mol. Pharmacol.* 81, 788–799.
- Rastinejad, F., Ollendorff, V., Polikarpov, I., 2015. Nuclear receptor full-length architectures: confronting myth and illusion with high resolution. *Trends Biochem. Sci.* 40, 16–24.
- Wallace, A.C., Laskowski, R.A., Thornton, J.M., 1995. LIGPLOT: a program to generate schematic diagrams of protein-ligand interactions. *Protein Eng.* 8, 127–134.
- Xu, H.E., Lambert, M.H., Montana, V.G., Plunket, K.D., Moore, L.B., Collins, J.L., Oplinger, J.A., Kliewer, S.A., Gampe, R.T., McKee, D.D., Moore, J.T., Willson, T.M., 2001. Structural determinants of ligand binding selectivity between the peroxisome proliferator-activated receptors. *Proc. Natl. Acad. Sci. U.S.A.* 98, 13919–13924.
- Xu, H.E., Stanley, T.B., Montana, V.G., Lambert, M.H., Shearer, B.G., Cobb, J.E., McKee, D.D., Galardi, C.M., Plunket, K.D., Nolte, R.T., Parks, D.J., Moore, J.T., Kliewer, S.A., Willson, T.M., Stimmel, J.B., 2002. Structural basis for antagonist-mediated recruitment of nuclear co-repressors by PPARalpha. *Nature* 415, 813–817.
- Zoete, V., Grosdidier, A., Michielin, O., 2007. Peroxisome proliferator-activated receptor structures: ligand specificity, molecular switch and interactions with regulators. *Biochim. Biophys. Acta* 1771, 915–925.